Arbitrarily massive sterile neutrinos at the neutrino factory

Davide Meloni[1], Jian Tang[2], Walter Winter[3]

Institut für Theoretische Physik und Astrophysik, Universität Würzburg, D-97074 Würzburg, Germany

Abstract. We study the effects of one additional sterile neutrino at the Neutrino Factory. On the one hand, we do not impose any constraint on the additional mass squared splitting, which is different from earlier discussions where LSND motivated $\mathcal{O}(1)$ eV^2 is always assumed. We find that a combination of near detectors and long baselines is good at searching for arbitrarily massive sterile neutrinos at the neutrino factory. On the other hand, we compare our sensitivities of mixing angles with the MINOS results where $|\Delta m^2_{41}| \gg |\Delta m^2_{31}|$ is assumed and the fast oscillations in the far detectors are averaged out.

Keywords: Neutrino oscillations
PACS: 14.60.Pq

Neutrino oscillation experiments have given us compelling evidence that active neutrinos are massive particles [1]. Assuming three-generation massive neutrinos, there are two characteristic mass squared splittings ($\Delta m^2_{31}, \Delta m^2_{21}$) and three mixing angles ($\theta_{12}, \theta_{13}, \theta_{23}$) as well as a CP violation phase $\delta_{\rm CP}$. Although we get good constraints on Δm^2_{21} and θ_{12}, $|\Delta m^2_{31}|$ and θ_{23} and an upper limit of θ_{13} by the global analysis of solar, atmospheric and reactor neutrino experiments [2], there are still unknown questions in the standard scenario: $\Delta m^2_{31} > 0$ (normal ordering) or $\Delta m^2_{31} < 0$ (inverted ordering); the value of θ_{13}, as there has been a recent hint for $\theta_{13} > 0$ [3], and whether there is CP violation (CPV) in the lepton sector. Neutrino Factory (NF) [4] is proposed as one of the best options to answer these questions. Physics with near detector configurations at NF have been discussed in Refs. [5, 6]. Recently a low energy version of NF is also been proposed with $E_\mu \sim 5$ GeV in Refs. [7, 8, 9, 10, 11, 12]. Apart from standard measurements, there has been the exceptional LSND measurement with an incompatible anomaly [13]. The simplest interpretation has been an additional sterile neutrino added to the standard picture with $|\Delta m^2_{41}| \gg |\Delta m^2_{31}|$. A global fit to all experimental data, however, is not in favor of this hypothesis [14], which means that more exotic scenarios would be required to describe this anomaly, such as a decaying sterile neutrino [15]. The recent results from MiniBooNE, however, suggest sterile neutrino oscillations in the antineutrino sector [16]. Note that the LSND interpretation requires significant mixings with the active neutrinos, whereas small ad-mixtures, even if $|\Delta m^2_{41}| \gg |\Delta m^2_{31}|$, are not excluded. Meanwhile, sterile neutrinos with $|\Delta m^2_{41}| \sim |\Delta m^2_{31}|$ or $|\Delta m^2_{41}| \sim \Delta m^2_{21}$, as they are motivated by a recent cosmological data analysis [17], have been hardly studied in the literature. In addition, Neutrino Factory is claimed to be a precision instrument not only because it can answer the unknown questions addressed above, but also because it can tell us the story beyond three flavor neutrino oscillation physics. Therefore, we discuss arbitrarily massive sterile neutrinos beyond LSND at the neutrino factory [18]. We consider the simplest case of only one additional sterile neutrino.

The four neutrino schemes can be categorized into two different classes: the 2+2 scheme, in which the solar and atmospheric mass squared splittings are separated by a new splitting, and the 3+1 scheme, in which the new mass eigenstate is added somewhere to the existing mass pattern. The 2+2 scheme is strongly disfavored by global fits [19, 20]. The 3+1 scheme, on the other hand, naturally recovers the standard picture in the case of small mixings. Therefore, we consider the 3+1 scheme only. We show the possible mass ordering of four neutrino eigenstates in Fig. 1. The arrow illustrates the new characteristic mass squared difference Δm^2_{41}. The four different scenarios correspond to $\Delta m^2_{31} > 0$, $\Delta m^2_{41} > 0$ (A), $\Delta m^2_{31} > 0$, $\Delta m^2_{41} < 0$ (B), $\Delta m^2_{31} < 0$, $\Delta m^2_{41} > 0$ (C), and $\Delta m^2_{31} < 0$, $\Delta m^2_{41} < 0$ (D). Unless noted explicitly, we show the results for scenario (A).

In addition, we have to keep in mind that the four neutrino scheme has to recover the standard picture once we switch off the small mixings between active and sterile neutrinos, while the global fits tell us that the mixings between active and sterile neutrinos must be small. Here we adopt an explicit parametrization:

$$\begin{aligned} U =& R_{34}(\theta_{34}, 0)\, R_{24}(\theta_{24}, 0)\, R_{14}(\theta_{14}, 0) \\ & R_{23}(\theta_{23}, \delta_3)\, R_{13}(\theta_{13}, \delta_2)\, R_{12}(\theta_{12}, \delta_1)\,. \end{aligned} \quad (1)$$

[1] davide.meloni@physik.uni-wuerzburg.de
[2] Speaker email: jtang@physik.uni-wuerzburg.de
[3] email: winter@physik.uni-wuerzburg.de

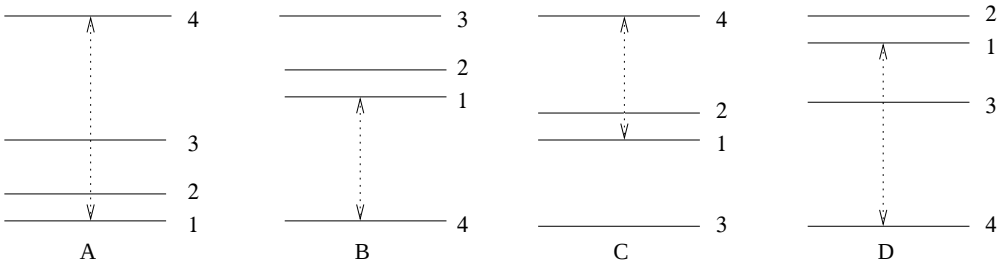

FIGURE 1. The mass ordering of four neutrino eigenstates (not to scale). The arrow illustrates the new characteristic mass squared difference Δm^2_{41}. The four different scenarios correspond to $\Delta m^2_{31} > 0$, $\Delta m^2_{41} > 0$ (A), $\Delta m^2_{31} > 0$, $\Delta m^2_{41} < 0$ (B), $\Delta m^2_{31} < 0$, $\Delta m^2_{41} > 0$ (C), and $\Delta m^2_{31} < 0$, $\Delta m^2_{41} < 0$ (D). The figure is taken from Ref. [18].

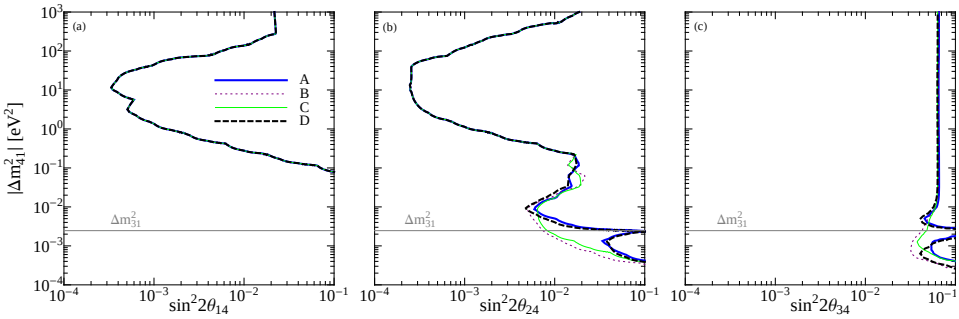

FIGURE 2. The exclusion limit for $\sin^2 2\theta_{i4}$–$\Delta m^2_{41} (i = 1,2,3)$ (region on r.h.s. of curves excluded). Here gives results of the standard IDS-NF (4000 km and 7500 km) setup with detectors for the four different mass orderings in Fig. 1; 90% CL (2 d.o.f.). The figure is based on Fig. 3 in Ref. [18].

This parametrization meets the above requirements easily. In Eq. (1), $R_{ij}(\theta_{ij},\ \delta_l)$ are the complex rotation matrices in the ij-plane. See Ref. [18] for definitions. This means that δ_2 becomes $\delta_{\rm CP}$ in the three flavor limit. Majorana phases are not shown due to their absence in the oscillation probabilities. The parametrization in Eq. (1) is the same to those used in Refs. [21, 22], and that in Ref. [23], since they fix their δ_2, corresponding to our δ_1, to zero.

To illustrate the effect from different mass orderings, as shown in Fig. 1, we display these figures for the standard IDS-NF (4000 km and 7500 km) setup in combination with near detectors in Fig. 2. Note that only the absolute value of the new mass squared difference is shown at the vertical axes. The upper peak hardly depends on the mass ordering. The lower (long-baseline) peak, which is only present in the middle and right panels, somewhat depends on the mass ordering. We identify two qualitatively different cases: In schemes A and D, the sensitivity is destroyed just at the value of Δm^2_{31}. In these cases, *cf.*, Fig. 1, mass eigenstates 3 and 4 are on top of each other, which means that there is no additional mass squared difference. The parameter correlations (marginalization over the unknown parameters) then destroy the sensitivity because the new mixing angles cannot be disentangled, in spite of the additional neutral current matter effect. This is different for schemes B and C, for which mass eigenstate 4 is on the opposite site of mass eigenstate 3. Although the absolute values of Δm^2_{41} and Δm^2_{31} are similar, these mass squared differences have different signs leading to different (charged current) matter effects.

To show a comparison of sensitivities, as shown in Fig. 3, we provide figures for exclusion limits of mixing angles where a 4000 km far detector at NF is simulated. In Ref. [23] the sensitivities of mixing angles were already discussed in terms of $|\Delta m^2_{41}| \gg |\Delta m^2_{31}|$ (in mass ordering A). We compare results at NF with theirs under the same assumptions for the combined fits in the θ_{34}–θ_{24} (a), θ_{23}–θ_{24} (b), and θ_{34}–θ_{23} (c) planes in Fig. 3. Note that the suppressed parameters are fixed, such as $\theta_{14} = 0$ and the phases, and that θ_{13} is fixed to two different values (not marginalized over). The best-fit values are also marked. Here we use the 4000 km baseline only. Obviously, the Neutrino Factory would reduce the allowed parameter space significantly, especially if θ_{13} is large. Note that the full marginalization would destroy the sensitivities.

In summary, we have discussed arbitrarily massive sterile neutrinos at the neutrino factory. We have found

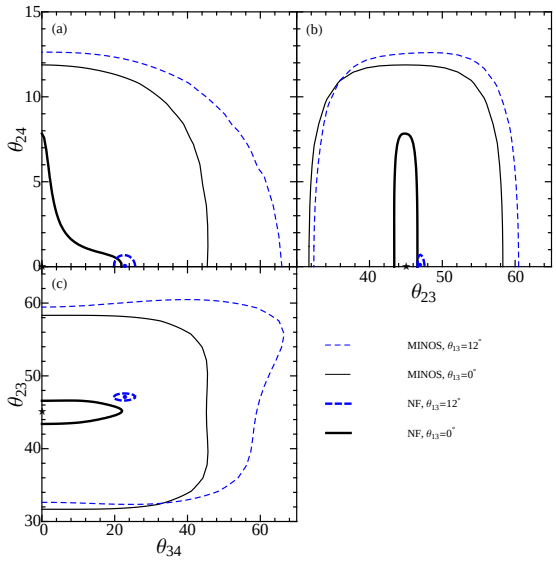

FIGURE 3. Exclusion limits in the θ_{34}–θ_{24} (a), θ_{23}–θ_{24} (b), and θ_{34}–θ_{23} (c) planes at the 90% CL. The different curves correspond to MINOS and the Neutrino Factory with $\Delta m^2_{41} = 1$ eV^2. Here only one NF far detector at 4000 km is used (without near detectors). All contours represent 90% confidence level. The solid curves assume $\theta_{13} = 0^\circ$, while the dashed curves assume $\theta_{13} = 12^\circ$. The best-fit values are marked in the figure, the one of θ_{24} is zero. The figure is taken from Ref. [18].

that there is a qualitative difference between the different mass orderings due to different matter effects. Meanwhile, there is a region corresponding to light sterile neutrinos in the atmospheric mass squared range which may not be extremely compelling but these bounds are very robust and independent of any special assumptions. Apart from the general constraints, we have compared our analysis to special cases with MINOS results in terms of $|\Delta m^2_{41}| \gg |\Delta m^2_{31}|$. The neutrino factory could provide the extremely good sensitivities.

JT appreciates good organizations and insightful discussions at NuFact10. JT is supported to attend the conference by DFG Research Training Group GRK 1147 Theoretical Astrophysics and Particle Physics.

REFERENCES

1. M. C. Gonzalez-Garcia, and M. Maltoni, *Phys. Rept.* **460**, 1–129 (2008), 0704.1800.
2. M. C. Gonzalez-Garcia, M. Maltoni, and J. Salvado, *JHEP* **04**, 056 (2010), 1001.4524.
3. G. L. Fogli, E. Lisi, A. Marrone, A. Palazzo, and A. M. Rotunno, *Phys. Rev. Lett.* **101**, 141801 (2008), 0806.2649.
4. International design study of the neutrino factory, http://www.ids-nf.org.
5. T. Abe, et al., *JINST* **4**, T05001 (2009), 0712.4129.
6. J. Tang, and W. Winter, *Phys. Rev.* **D80**, 053001 (2009), arXiv:0903.3039.
7. S. Geer, O. Mena, and S. Pascoli, *Phys. Rev.* **D75**, 093001 (2007), hep-ph/0701258.
8. A. D. Bross, M. Ellis, S. Geer, O. Mena, and S. Pascoli, *Phys. Rev.* **D77**, 093012 (2008), 0709.3889.
9. P. Huber, and W. Winter, *Phys. Lett.* **B655**, 251–256 (2007), 0706.2862.
10. A. Bross, et al., *Phys. Rev.* **D81**, 073010 (2010), 0911.3776.
11. E. Fernandez Martinez, T. Li, S. Pascoli, and O. Mena, *Phys. Rev.* **D81**, 073010 (2010).
12. J. Tang, and W. Winter, *Phys. Rev.* **D81**, 033005 (2010), 0911.5052.
13. A. Aguilar, et al., *Phys. Rev.* **D64**, 112007 (2001), hep-ex/0104049.
14. M. Maltoni, and T. Schwetz, *Phys. Rev.* **D76**, 093005 (2007), 0705.0107.
15. S. Palomares-Ruiz, S. Pascoli, and T. Schwetz, *JHEP* **09**, 048 (2005), hep-ph/0505216.
16. A. A. Aguilar-Arevalo, et al. (2010), 1007.1150.
17. J. Hamann, S. Hannestad, G. G. Raffelt, I. Tamborra, and Y. Y. Y. Wong (2010), 1006.5276.
18. D. Meloni, J. Tang, and W. Winter, *Phys. Rev.* **D82**, 093008 (2010), 1007.2419.
19. M. Maltoni, T. Schwetz, M. A. Tortola, and J. W. F. Valle, *Phys. Rev.* **D67**, 013011 (2003), hep-ph/0207227.
20. M. Maltoni, T. Schwetz, M. A. Tortola, and J. W. F. Valle, *New J. Phys.* **6**, 122 (2004), hep-ph/0405172.
21. A. Donini, M. Maltoni, D. Meloni, P. Migliozzi, and F. Terranova, *JHEP* **12**, 013 (2007), 0704.0388.
22. A. Donini, K.-i. Fuki, J. Lopez-Pavon, D. Meloni, and O. Yasuda, *JHEP* **08**, 041 (2009), 0812.3703.
23. P. Adamson, et al., *Phys. Rev.* **D81**, 052004 (2010), 1001.0336.